This is an open access article published under a Creative Commons Non-Commercial No Derivative Works (CC-BY-NC-ND) Attribution License, which permits copying and redistribution of the article, and creation of adaptations, all for non-commercial purposes.

Macromolecules

Article

Cite This: Macromolecules 2019, 52, 5948−5954

pubs.acs.org/Macromolecules

# Physical Ageing of Polystyrene: Does Tacticity Play a Role?

Kalouda Grigoriadi,[†,‡] Jeroen B. H. M. Westrik,[†] Georgios G. Vogiatzis,[†,‡] Lambèrt C. A. van Breemen,[†] Patrick D. Anderson,[†] and Markus Hütter*[,†]

[†]Polymer Technology, Department of Mechanical Engineering, Eindhoven University of Technology, P.O. Box 513, 5600 MB Eindhoven, The Netherlands

[‡]Dutch Polymer Institute, P.O. Box 902, 5600 AX Eindhoven, The Netherlands

**ABSTRACT:** The ageing kinetics of amorphous atactic (a-PS), isotactic (i-PS), and syndiotactic (s-PS) polystyrene were studied by means of flash-differential scanning calorimetry. The specimens were aged for up to 2 h at six different ageing temperatures: the optimum ageing temperature, that is, the temperature at which the enthalpy overshoot at the glass transition is maximal for the given elapsed time, and five ageing temperatures ranging from 20 to 80 K below the optimum ageing temperature. A logarithmic increase of the enthalpy overshoot with ageing time is observed for specimens at their optimum ageing temperatures. For temperatures significantly lower than the optimum, there is a range where the enthalpy overshoot is constant, but for higher temperatures (still below the optimum), a logarithmic increase is also observed. Moreover, the ageing kinetics appear to depend on tacticity, with s-PS and i-PS exhibiting the slowest and fastest ageing kinetics, respectively, and a-PS exhibiting ageing kinetics between these two extremes.

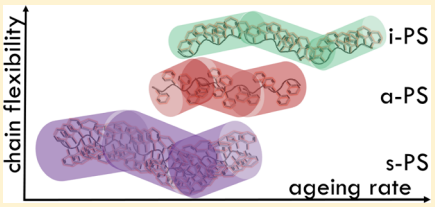


## INTRODUCTION

Glasses are known to be far from their thermodynamic equilibrium, and their structural relaxation toward equilibrium, via a sequence of molecular rearrangements, is known as physical ageing.[1] Physical ageing of polymeric glasses is known to affect the material properties, like the mechanical[2,3] or gas-transport properties,[4] posing limitations on their applications. A lot of studies have been conducted on the influence of physical ageing of glassy polymers on yielding,[1−3,5,6] creep,[7−9] volume relaxation,[8,10−14] enthalpy changes,[9,11,15−17] molecular-scale dynamics,[18−21] and structural changes.[22−24] However, the connection between the molecular structure and the ageing kinetics has not yet been established.

Despite the fact that numerous techniques are employed to study the large number of properties affected by physical ageing in glassy polymers, only one of them can cool and heat the material rapidly enough to allow probing of the ageing kinetics by starting from a "true" rejuvenated amorphous state. This technique is flash-differential scanning calorimetry (flash-DSC) in which ultra-high heating and cooling rates (>100 000 K/min) can be applied.[25] The majority of the ageing studies with flash-DSC involve measurements concerning a single material such as atactic polystyrene (a-PS),[26−30] polycarbonate (PC),[29] poly lactic-acid,[31,32] and others.[33,34] Until now, there are only very few studies investigating the effect of tacticity on the ageing kinetics[35] of glassy amorphous polymers. The main reason for the lack of studies is that syndiotactic and isotactic polymers crystallize under normal cooling rates, resulting in a semicrystalline material. For polystyrenes, there is another limiting factor next to the high crystallization rate[36] of s-PS, namely, its melting temperature is very close to its degradation temperature, which makes the preparation of an amorphous sample in oxygen atmosphere impossible because the material starts to degrade before the crystallinity is erased. The high crystallization rate can be tackled by the high cooling rate that flash-DSC offers, and the complete melting of crystals before the material degrades has been taken care of by using a nitrogen atmosphere during the measurement.

In this work, we study the effect of tacticity on the ageing kinetics at high and low ageing temperatures for atactic, isotactic, and syndiotactic polystyrene using flash-DSC in their glassy state.

## METHODOLOGY

**Materials.** Atactic and syndiotactic PS (Figure 1) with syndio contents ≥90% were bought in powder and pellet forms, respectively, from Polymer Source.[37] Isotactic PS (Figure 1) with 90% isotactic content was bought in the powder form from Scientific Polymer Products.[38] The corresponding molecular weights and polydispersity indices (PDIs) are listed in Table 1.

**Differential Scanning Calorimetry.** *Flash-Differential Scanning Calorimetry.* Experiments were carried out in Mettler Toledo Flash-DSC 1 equipped with a Huber TC100 intracooler under a constant flow of dry nitrogen using UFS1 sensors.

*Differential Scanning Calorimetry.* Experiments were carried out in a Mettler-Toledo 823e/700 module with a Cryostat intracooler using a 50 μL aluminum pan under a constant flow of dry nitrogen.

**Received:** May 21, 2019
**Revised:** July 2, 2019
**Published:** July 31, 2019


© 2019 American Chemical Society

DOI: 10.1021/acs.macromol.9b01042
Macromolecules 2019, 52, 5948−5954

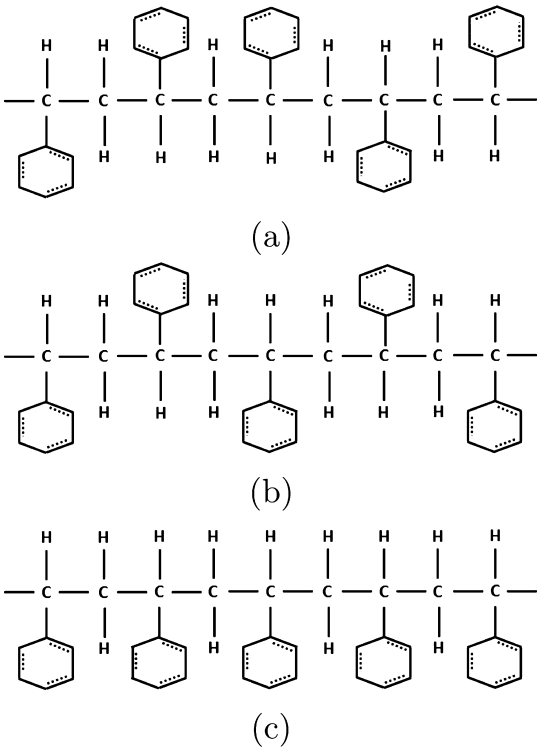


**Figure 1.** Stereochemistry of (a) atactic, (b) syndiotactic, and (c) isotactic polystyrene.

**Table 1. Number-Average Molecular Weight $M_n$ and PDI of the Polystyrene Samples**

| sample | $M_n$ (kg/mol) | PDI (-) |
|---|---|---|
| a-PS | 412 | 1.05 |
| s-PS | 250 | 3.5 |
| i-PS | 400 | 2 |

**Sample Preparation.** For the flash-DSC measurements, very small specimens of material of approximately 30−170 ng were cut and put onto the sensor with the use of an eyelash. For the conventional DSC, the powder-form samples were put in an aluminum pan with a mass between 5 and 10 mg.

**Estimation of Sample Mass.** In the case of the flash-DSC measurements, the sample mass cannot be measured with a conventional scale because the weight is too small (nanogram). For semicrystalline materials, the mass can be estimated as follows. A sample of known mass is cooled and heated in conventional DSC at 20 K/min, and the specific melting enthalpy ($\Delta h_m$) is calculated by peak integration of the heating curve. Afterward, a sample of unknown mass is cooled at 20 K/min and heated at 1000 K/s in the flash-DSC equipment. The melting enthalpy ($\Delta H_m$) is calculated from the heating curve, and the mass of the flash-DSC sample can be determined by

$$m_{sc} = \frac{\Delta H_m}{\Delta h_m} \quad (1)$$

In the case of amorphous polymers, the sample mass can be estimated by using the method of Cebe et al.,[39] employing the liquid heat capacity from flash-DSC (cooling rate 1000 K/s) and the specific heat-capacity from the ATHAS bank.[40] The sample mass $m_{am}$ is determined by

$$m_{am} = \frac{C_{p_{FDSC}}}{c_{p_{DSC}}} \quad (2)$$

where $C_{p_{FDSC}}$ is the heat capacity obtained from the flash-DSC experiments far above the glass transition temperature and $c_{p_{DSC}}$ is the specific liquid heat capacity taken from the ATHAS bank. The validity of the method is confirmed by applying both eqs 1 and 2 to a semicrystalline sample. The error between the two mass-estimation methods is found to be about 5%.

**Methods.** In order to study the ageing kinetics of the selected materials, the temperature protocol shown in Figure 2

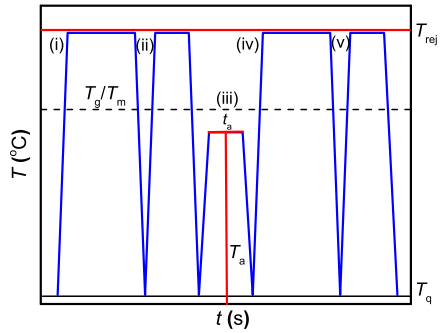


**Figure 2.** Schematic representation of the flash-DSC heating protocol: (i) Heating above $T_g$ or $T_m$, (ii) reference-state heating curve, (iii) isothermal ageing for ageing time $t_a$ and at temperature $T_a$, (iv) aged-state heating curve, and (v) reference-state heating curve. The values of rejuvenation, $T_{rej}$, and end-quenching temperature, $T_q$, are provided in Table 2.

was used. The following steps can be identified: Step i: the sample was heated well above $T_g$ (a-PS) or $T_m$ (s-PS and i-PS) at a rejuvenation temperature $T_{rej}$ (Table 2 and Figure 2) in order to erase its thermomechanical history (i.e., thermal rejuvenation). Step ii: The sample was rapidly quenched at a cooling rate of 1000 K/s to an end-quenching temperature $T_q$ well below $T_g$, and subsequently heated rapidly (heating rate: 1000 K/s) above $T_g$ to obtain the heating curve which serves as a reference state. Step iii: The sample is rapidly quenched (1000 K/s) and then heated (1000 K/s) to the chosen ageing temperature, $T_a$, and held at that temperature for a specific ageing time $t_a$. Step iv: The sample was quenched rapidly (1000 K/s) at 25 °C for ageing temperatures higher than 25 and 0 °C for ageing temperatures below 25 °C to capture the aged state and heated rapidly (1000 K/s) above $T_g$ (or $T_m$) to obtain the endothermic peak caused by ageing, and to thermally rejuvenate the sample for the next measurement. Step v: One more cycle of quenching and heating was

**Table 2. Glass-Transition Temperature, $T_g$, and Melting Temperature, $T_m$, for a-PS, s-PS, and i-PS, Measured during Heating with a Heating Rate of 1000 K/s, and Rejuvenation, $T_{rej}$, and End-Quenching Temperatures, $T_q$[a]**

| sample | $T_g$ (°C) | $T_m$ (°C) | $T_{rej}$ (°C) | $T_q$ (°C) |
|---|---|---|---|---|
| a-PS | 128 | | 190 | 25 and 0 |
| s-PS | 124 | 270 | 310 | 25 and 0 |
| i-PS | 126 | 240 | 270 | 25 and 0 |

[a]The end-quenching temperature is 25 °C for ageing temperatures higher than 25 and 0 °C for ageing temperatures below 25 °C.



DOI: 10.1021/acs.macromol.9b01042
Macromolecules 2019, 52, 5948−5954

performed to validate the rejuvenated state of the polymer (heating curve).

**Analysis.** The analysis of experimental data concerning the cooling-rate dependence of $T_g$ and physical ageing can be analyzed in terms of enthalpy loss ($\Delta H_a$) or the fictive temperature ($T_f$).[29] Tool[41] defined $T_f$ as a measure of the glass structure. The intersection of the extrapolated glass line and the extrapolated liquid line determines $T_f$. The $T_f$ of an aged glass is related to the change in enthalpy with ageing[29]

$$\Delta H_a = \int_{T_{f0}}^{T_f} \Delta C_p \, dT \tag{3}$$

where $\Delta H_a$ is the enthalpy loss upon ageing, $T_f$ is the fictive temperature of the aged glass, $T_{f0}$ is the fictive temperature of the unaged glass, and $\Delta C_p$ is the step change in heat capacity. During physical ageing, $T_{f0}$ decreases to an equilibrium value, while $\Delta H_a$ increases from a zero value to the equilibrium enthalpy value.[29] We chose to analyze our data using the $\Delta H_a$ changes. Both types of analysis will yield identical conclusions/observations. The analysis procedure is described below.

*Fitting a Straight Line to the Liquid Regime.*[29] The calculation of the enthalpy overshoot of the aged specimen (i.e., the integral under the $C_p(T)$-curve) relies on drawing an unbiased liquid line, especially when a large overshoot is present. Thus, each heating scan was superposed with the subsequent scan of a freshly quenched specimen. The liquid line was determined as the best linear fit of the $C_p(T)$-curve at high temperatures, away from the enthalpy overshoot and the transition region. A consistent liquid line is crucial for calculating the integral under the $C_p(T)$-curve. As shown in Figure 3, the enthalpy overshoot of the aged specimen is

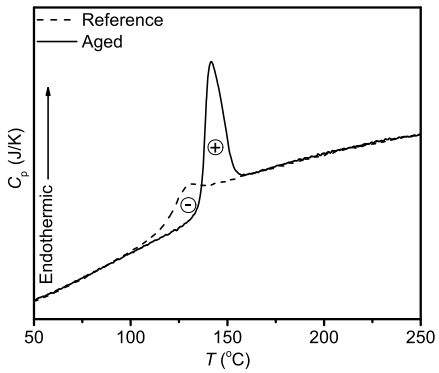


**Figure 3.** Representative curve for the calculation of the enthalpy loss $\Delta H_a$ upon ageing, according to the Petrie method.[42]

calculated in between the point where the $C_p(T)$-curve departs from the linear liquid line till the point where it intersects again. This integral is considered positive. Then, we apply the same procedure to the rejuvenated sample and subtract its integral from that of the aged one.

*Determination of Excess Enthalpy.* The excess enthalpy was determined using the method of Petrie[42] in which the enthalpy loss $\Delta H_a$ upon ageing is calculated by the difference of the integrated $C_p(T)$-curves of the aged and reference (rejuvenated) material (Figure 3)

$$\Delta H_a = \int_{T_a}^{T_c} (C_p)_{aged} \, dT - \int_{T_a}^{T_c} (C_p)_{ref} \, dT \tag{4}$$

Two measurements per sample are conducted for each ageing time and temperature.

**Sensor Corrections.** Conditioning and correction were performed on the flash-DSC chip sensors before the sample is positioned on the sensor according to the manufacturers recommended protocol. No additional temperature corrections were applied because the calibration by the manufacturer was found to have an error of about 0.6−0.7 K.[43]

## RESULTS

In Figure 4, the flash-DSC heating curves for atactic, syndiotactic, and isotactic amorphous PS annealed at various

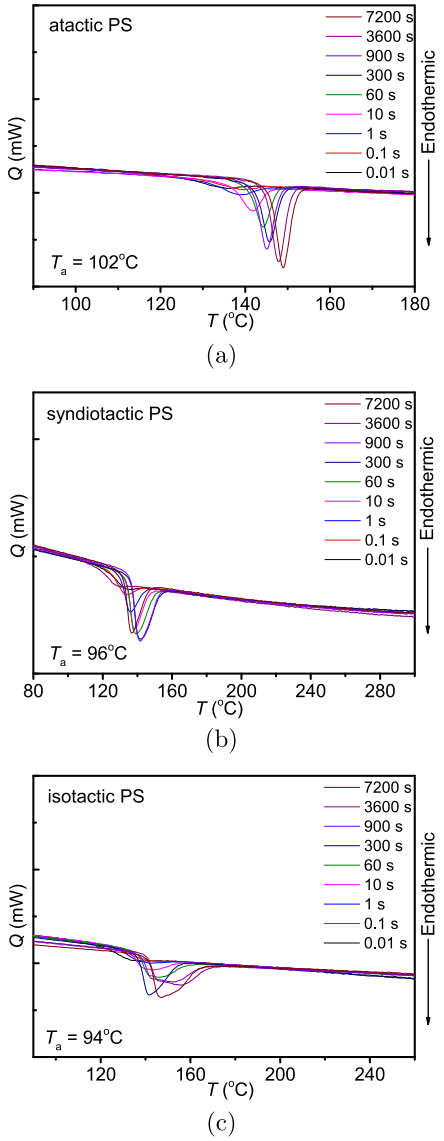


**Figure 4.** Heat flow $Q$ versus temperature $T$ for (a) a-PS, (b) s-PS, and (c) i-PS, for various ageing times.

ageing temperatures and ageing times are shown. It can be seen that the area of the endothermic peak as well as the temperature where the endothermic peak appears are increasing with the ageing time. Also, the absence of a melting peak, as a result of the high cooling rate (1000 K/s) in the case of semicrystalline polymers, validates the fact that the samples are in an amorphous state (Figure 4).



DOI: 10.1021/acs.macromol.9b01042
*Macromolecules* 2019, 52, 5948−5954

We study the effect of ageing temperature $T_a$ on the excess enthalpy $\Delta H_{tot} - \Delta H_{rej}$ for an annealing time of 10 min for atactic, syndiotactic, and isotactic amorphous PS (Figure 5).

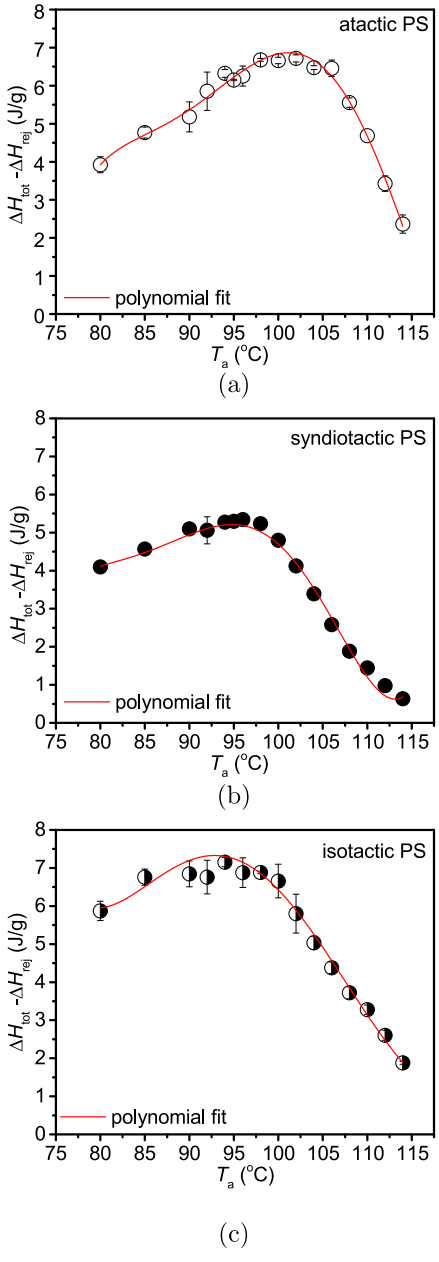


**Figure 5.** Excess enthalpy, $\Delta H_{tot} - \Delta H_{rej}$, vs annealing temperature, $T_a$, for (a) a-PS, (b) s-PS, and (c) i-PS. The ageing time is $t_a$ = 10 min. Lines represent the polynomial fits (see main text).

Figure 5a shows that for a-PS, the excess enthalpy increases linearly with temperature where it reaches a maximum at around 102 °C (≈26 K below the glass-transition temperature). After this temperature, the enthalpy overshoot decreases linearly. Similarly, the s-PS (Figure 5b) excess enthalpy follows a linear increase with an optimum at ≈96 °C, (≈28 K below $T_g$) and a decrease after this optimum as well. i-PS (Figure 5c) has a similar behavior with an optimum enthalpy overshoot at ≈94 °C (32 K below $T_g$). Based on these results, we choose the temperature in which each polymer shows the largest overshoot as the optimum ageing temperature ($T_{opt}$), determined by fitting a polynomial of the fifth order to the $\Delta H_{tot} - \Delta H_{rej}$ versus $T_a$ data (Figure 5). We perform measurements also at 20 K ($T_{opt\text{-}20K}$), 30 K ($T_{opt\text{-}30K}$), 40 K ($T_{opt\text{-}40K}$), 60 K ($T_{opt\text{-}60K}$), and 80 K ($T_{opt\text{-}80K}$) below $T_{opt}$ for all specimens. It is also noted that the behavior displayed in Figure 5 on the left and right sides of the maximum, $T_{opt}$, is asymmetric; similar observations have been made earlier.[44] The fact that the left side changes only smoothly with temperature is indicative of non-$\alpha$-processes being relevant in this regime.

In Figure 6, the excess enthalpy ($\Delta H_{tot} - \Delta H_{rej}$) as a function of the ageing time for the various ageing temperatures

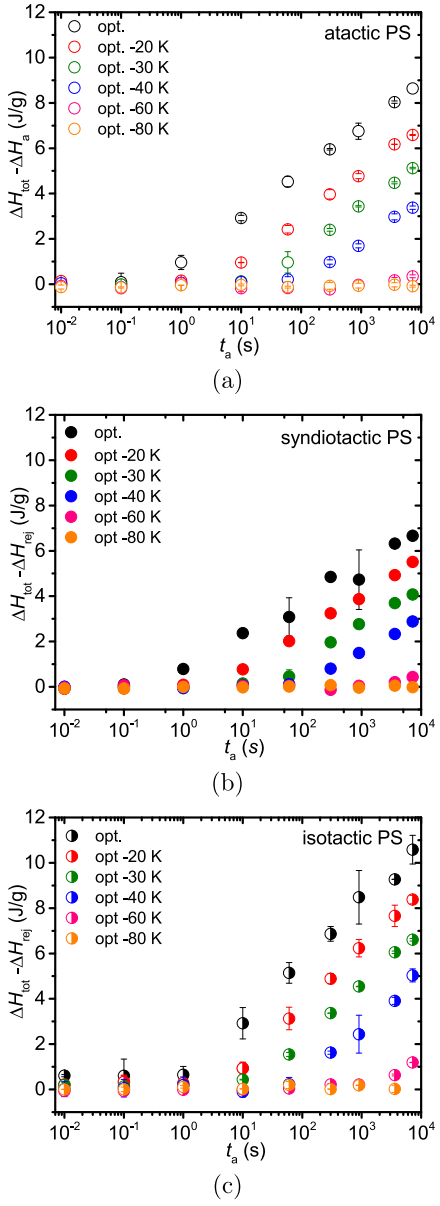


**Figure 6.** Excess enthalpy, $\Delta H_{tot} - \Delta H_{rej}$, vs ageing time, $t_a$, for (a) a-PS, (b) s-PS, and (c) i-PS.

for atactic, syndiotactic, and isotactic PS is shown. It can be seen that $\Delta H_{tot} - \Delta H_{rej}$ follows a logarithmic increase with time for the optimum ageing temperatures. For very short ageing times (≤0.1 s), the $\Delta H_{tot} - \Delta H_{rej}$ for the three PS specimens is close to zero. For longer ageing times (≥10 s), the excess enthalpy shows a logarithmic increase for all



DOI: 10.1021/acs.macromol.9b01042
*Macromolecules* 2019, 52, 5948−5954

specimens. At ageing temperatures below the optimum (Figure 6), it can be observed that the increase of $\Delta H_{tot} - \Delta H_{rej}$ does not follow a logarithmic increase and is reduced compared to that for long ageing times. Similar to the observations for maximum ageing temperature for short ageing times, the enthalpy overshoot observed for the three PS specimens is close to zero.

Using time−temperature superposition, an activation energy can be determined. In Figure 7, the $\Delta H_{tot} - \Delta H_{rej}$ curves are shifted horizontally along the logarithmic ageing-time axis, taking $T_{opt}$ as a reference. The good superposition of lines allows calculating the activation energy by plotting the logarithmic shift-factor ($a_T$) as a function of temperature and obtaining an Arrhenius plot for temperatures from $T_{opt\text{-}40K}$ to $T_{opt\text{-}20K}$. The activation energies $E_a$ for a-PS, s-PS, and i-PS calculated from the slope ($E_a/R$, where $R$ is the gas constant) in Figure 8 are found to be (166.6 ± 4.0) kJ/mol for a-PS,

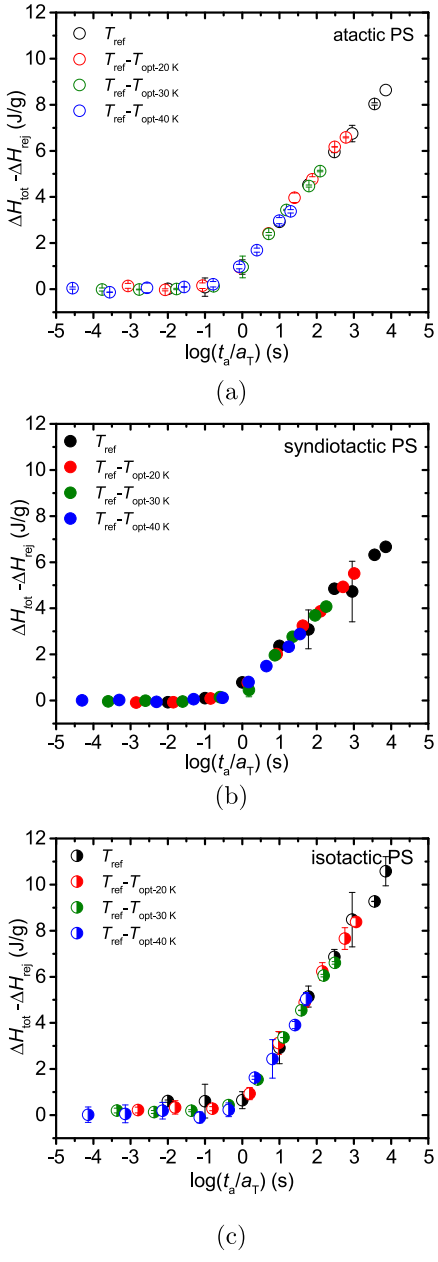


**Figure 7.** Excess enthalpy obtained from time−temperature superposition using the optimum ageing temperature as the reference, $T_{ref} = T_{opt}$, for (a) a-PS, (b) s-PS, and (c) i-PS.

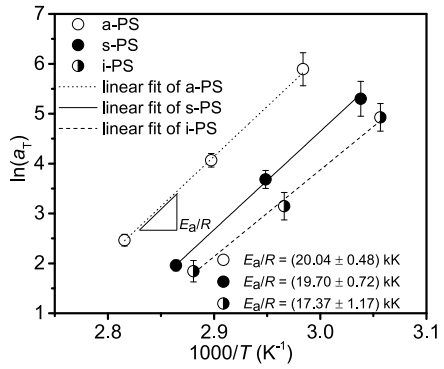


**Figure 8.** Arrhenius plot of the shift factor, $a_T$, for i-PS (half-filled circles), s-PS (filled circles), and a-PS (empty circles). The activation energy is represented by the slope of the lines.

(163.8 ± 6.0) kJ/mol for s-PS and (144.4 ± 9.7) kJ/mol for i-PS. Even if we take the lowest values for $E_a/R$ for a-PS and s-PS, we cannot reach the highest value for i-PS. This indicates that despite the differences being subtle, they are by no means negligible.

The slope in the Arrhenius plot (Figure 8) for a-PS calculated in this work has a value of around 20 kK, while the slope calculated in the work of Koh and Simon[43] has a value of 13 kK. Considering that in this work, we used a limited temperature range for the construction of the Arrhenius plot in Figure 8 compared to the work of Koh and Simon,[43] errors may have been introduced because of the errors in the shift factors. Despite these differences, the activation energies measured by flash-DSC are significantly smaller than the ones typically reported in the literature for the $\alpha$-process,[45] a fact that was also noted earlier.[46] The relatively small activation energies are, again, supporting the idea that non-$\alpha$-processes are relevant for the low-temperature behavior of the glass.

Furthermore, we quantify the ageing rate from the slope of $\Delta H_{tot} - \Delta H_{rej}$ in the range where it exhibits a linear increase with respect to the logarithm of time

$$R_{ag} = \frac{d(\Delta H_{tot} - \Delta H_{rej})}{d(\ln t_a)} \quad (5)$$

In Figure 9, the ageing rate, $R_{ag}$, is plotted as a function of the ageing temperature $T_a$. At $T_{opt\text{-}80K}$, $R_{ag}$ is close to zero,

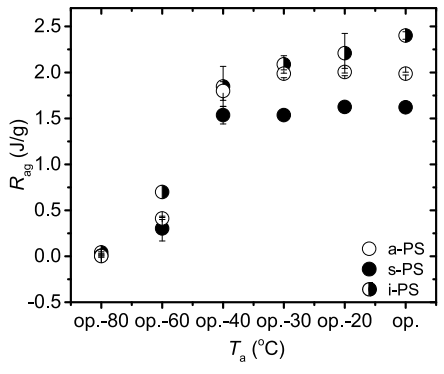


**Figure 9.** Ageing rate ($R_{ag}$) as a function of ageing temperature for i-PS (half-filled circles), s-PS (filled circles), and a-PS (empty circles).



DOI: 10.1021/acs.macromol.9b01042
Macromolecules 2019, 52, 5948−5954

increases slightly with ageing temperature at $T_{opt\text{-}60K}$, and has a large increase at $T_{opt\text{-}40K}$. The ageing rates for i-PS, a-PS, and s-PS are comparable for temperatures from $T_{opt\text{-}80K}$ to $T_{opt\text{-}40K}$. In addition, a-PS exhibits higher ageing rates than s-PS for temperatures above $T_{opt\text{-}40K}$, where i-PS has the highest ageing rate of all specimens at the optimum $T_a$.

## DISCUSSION

PS[15,47] as well as other glassy polymers such as PC[48,49] and PVC[50] have been reported to have logarithmic enthalpy overshoot increase at high-temperature ageing. For ageing at the optimum ageing temperature, the enthalpy overshoot increases logarithmically with time. For ageing temperatures below the optimum ageing temperatures, ageing shows a non-logarithmic dependence on time. The farther the ageing temperature of the material is from its optimum ageing temperature, the longer the material stays in an arrested state until it shows a logarithmic increase in excess enthalpy with time (Figure 6), similar to the enthalpy increase which has been reported for PC.[48]

While all materials exhibit the same ageing mechanisms for all temperatures (logarithmic increase of excess enthalpy with $T_{opt}$ and delayed increase of the excess enthalpy with ageing at temperatures far below optimum), it is worth noting the effect of tacticity on the ageing rate (Figure 9). Specifically, a-PS and i-PS show a similar ageing rate for temperatures from $T_{opt\text{-}40K}$ to $T_{opt\text{-}20K}$, while at the optimum ageing temperature, the fastest ageing kinetics are observed for i-PS. s-PS shows the slowest ageing kinetics between the three polymers, specifically for temperatures from $T_{opt\text{-}40K}$ to $T_{opt}$.

We believe that the reason behind the difference of the rate at which a-PS, s-PS, and i-PS age is related to the difference in chain flexibility of those polymers. Nakaoki and Kobayashi[51] studied, by solid-state high-resolution $^{13}C$ NMR, the gauche content of amorphous atactic, syndiotactic, and isotactic PS, finding 27.9, 25.0, and 34.3%, respectively. Based on their results, they concluded that i-PS is more likely to have fewer trans sequences, which leads to a shorter random coil and to a smaller characteristic ratio ($C_\infty$). This has been confirmed by small-angle neutron scattering studies which have revealed that the characteristic ratio is $C_\infty^{s\text{-}PS} > C_\infty^{a\text{-}PS} > C_\infty^{i\text{-}PS}$, that points out that the stiffest chain is the one of s-PS.[52] Specifically, the $C_\infty^{s\text{-}PS}$ value is 7.9 to 13 for increasing $M_w$ from 214 000 to 380 000 g/mol.[53] The $C_\infty^{a\text{-}PS}$ value is 6.7 to 9.6 for increasing $M_w$ from 325 000 to 500 000 g/mol, and the $C_\infty^{i\text{-}PS}$ values are 4.9 and 5 for $M_w$ = 254 000 and 500 000 g/mol, respectively.[53] Syndiotactic sequences make the polymer chain rigid[54] and slow down the reorganization of the chains, which consequently leads to slower ageing kinetics, as it has been shown in our measurements (Figure 9). Tensile creep measurements on polyimide Kapton-H and cellulose acetate butyrate ester have also suggested that the ageing kinetics are slower for the more rigid polymers.[55]

As shown above, the rate of ageing decreases with increasing chain stiffness, s-PS ageing significantly slower than i-PS. This is in stark contrast to the behavior of these two materials in crystallization; s-PS crystallizes about hundred times faster than i-PS because of differences in the conformation of the C–C backbone and the work of chain folding.[56] This contrast shows that ageing and crystallization are clearly distinct phenomena.

## CONCLUSIONS

The effect of tacticity on the ageing kinetics of glassy amorphous PS was investigated by flash-DSC. Our results show that the tacticity does have an effect on the physical ageing kinetics, with syndiotactic and isotactic PS showing the two extremes, slow and fast ageing kinetics, respectively, and atactic PS showing ageing kinetics between these two extremes.

The enthalpy overshoot of all PS specimens follows a logarithmic increase with ageing time at their optimum ageing temperature. For temperatures far below its optimum, there is a range, different for each specimen, where the enthalpy overshoot is constant, whereas at higher temperatures (but still below the optimum temperature), it also shows a logarithmic increase. In addition, the activation energy for i-PS is found to be the lowest, while the activation energies of a-PS and s-PS have the same values within experimental error. The results reported in this paper indicate that non-$\alpha$-processes are relevant for the low-temperature behavior of the glass.

## AUTHOR INFORMATION


### Corresponding Author

*E-mail: M.Huetter@tue.nl. Phone: +31 40-247 2486.

### ORCID

Kalouda Grigoriadi: 0000-0001-6020-4679

Lambèrt C. A. van Breemen: 0000-0002-0610-1908

Markus Hütter: 0000-0002-8161-9002


### Notes

The authors declare no competing financial interest.

## ACKNOWLEDGMENTS

This research forms part of the research programs of the Dutch Polymer Institute (DPI), projects #745t, #745ft14 and #820.

## REFERENCES


(1) Struik, L. C. E. Physical aging in plastics and other glassy materials. *Polym. Eng. Sci.* **1977**, *17*, 165–173.

(2) Van Melick, H. G. H.; Govaert, L. E.; Raas, B.; Nauta, W. J.; Meijer, H. E. H. Kinetics of ageing and re-embrittlement of mechanically rejuvenated polystyrene. *Polymer* **2003**, *44*, 1171–1179.

(3) Huu, C. H.; Vu-Khanh, T. Effects of physical aging on yielding kinetics of polycarbonate. *Theor. Appl. Fract. Mech.* **2003**, *40*, 75–83.

(4) Laot, C. M.; Marand, E.; Schmittmann, B.; Zia, R. K. P. Effects of cooling rate and physical aging on the gas transport properties in polycarbonate. *Macromolecules* **2003**, *36*, 8673–8684.

(5) Sell, C. G.; McKenna, G. B. Influence of physical ageing on the yield response of model DGEBA/poly (propylene oxide) epoxy glasses. *Polymer* **1992**, *33*, 2103–2113.

(6) Chow, T. Stress-strain behaviour of physically ageing polymers. *Polymer* **1993**, *34*, 541–545.

(7) Soloukhin, V. A.; Brokken-Zijp, J. C. M.; van Asselen, O. L. J.; de With, G. Physical aging of polycarbonate: Elastic modulus, hardness, creep, endothermic peak, molecular weight distribution, and infrared data. *Macromolecules* **2003**, *36*, 7585–7597.

(8) Shelby, M. D.; Wilkes, G. L. The effect of molecular orientation on the physical ageing of amorphous polymers-dilatometric and mechanical creep behaviour. *Polymer* **1998**, *39*, 6767–6779.

(9) Liu, L. B.; Yee, A. F.; Gidley, D. W. Effect of cyclic stress on enthalpy relaxation in polycarbonate. *J. Polym. Sci., Part B: Polym. Phys.* **1992**, *30*, 221–230.

(10) Pixa, R.; Le Dû, V.; Wippler, C. Dilatometric study of deformation induced volume increase and recovery in rigid PVC. *Colloid Polym. Sci.* **1988**, *266*, 913–920.

(11) Burgess, S. K.; Mubarak, C. R.; Kriegel, R. M.; Koros, W. J. Physical aging in amorphous poly (ethylene furanoate): Enthalpic




DOI: 10.1021/acs.macromol.9b01042
*Macromolecules* 2019, 52, 5948–5954

recovery, density, and oxygen transport considerations. *J. Polym. Sci., Part B: Polym. Phys.* **2015**, *53*, 389−399.
(12) Huang, Y.; Wang, X.; Paul, D. Physical aging of thin glassy polymer films: free volume interpretation. *J. Membr. Sci.* **2006**, *277*, 219−229.
(13) Wang, B.; Gong, W.; Liu, W. H.; Wang, Z. F.; Qi, N.; Li, X. W.; Liu, M. J.; Li, S. J. Influence of physical aging and side group on the free volume of epoxy resins probed by positron. *Polymer* **2003**, *44*, 4047−4052.
(14) Cangialosi, D.; Schut, H.; Van Veen, A.; Picken, S. J. Positron annihilation lifetime spectroscopy for measuring free volume during physical aging of polycarbonate. *Macromolecules* **2003**, *36*, 142−147.
(15) Hourston, D. J.; Song, M.; Hammiche, A.; Pollock, H. M.; Reading, M. Modulated differential scanning calorimetry: 2. Studies of physical ageing in polystyrene. *Polymer* **1996**, *37*, 243−247.
(16) Kubota, Y.; Fukao, K.; Saruyama, Y. Heat flows on the heating process after aging of glassy poly (methyl methacrylate) measured by temperature modulated differential scanning calorimeter. *Thermochim. Acta* **2005**, *431*, 149−154.
(17) Berens, A. R.; Hodge, I. M. Effects of annealing and prior history on enthalpy relaxation in glassy polymers. 1. Experimental study on poly(vinyl chloride). *Macromolecules* **1982**, *15*, 756−761.
(18) Casalini, R.; Roland, C. M. Aging of the secondary relaxation to probe structural relaxation in the glassy state. *Phys. Rev. Lett.* **2009**, *102*, 035701.
(19) Wypych, A.; Duval, E.; Boiteux, G.; Ulanski, J.; David, L.; Seytre, G.; Mermet, A.; Stevenson, I.; Kozanecki, M.; Okrasa, L. Physical aging of atactic polystyrene as seen by dielectric relaxational and low-frequency vibrational Raman spectroscopies. *J. Non-Cryst. Solids* **2005**, *351*, 2593−2598.
(20) Lunkenheimer, P.; Wehn, R.; Loidl, A. Dielectric spectroscopy on aging glasses. *J. Non-Cryst. Solids* **2006**, *352*, 4941−4945.
(21) Wehn, R.; Lunkenheimer, P.; Loidl, A. Broadband dielectric spectroscopy and aging of glass formers. *J. Non-Cryst. Solids* **2007**, *353*, 3862−3870.
(22) Heymans, N. FTIR investigation of structural modification of polycarbonate during thermodynamical treatments. *Polymer* **1997**, *38*, 3435−3440.
(23) Pan, P.; Zhu, B.; Dong, T.; Yazawa, K.; Shimizu, T.; Tansho, M.; Inoue, Y. Conformational and microstructural characteristics of poly(L-lactide) during glass transition and physical aging. *J. Chem. Phys.* **2008**, *129*, 184902.
(24) Lu, J.; Wang, Y.; Shen, D. Infrared spectroscopic and modulated differential scanning calorimetric study of physical aging in bisphenol-A polycarbonate. *Polym. J.* **2000**, *32*, 610−615.
(25) Schawe, J. E. K.; Pogatscher, S. In *Fast Scanning Calorimetry*; Schick, J., Mathod, D., Eds.; Springer International Publishing, 2016; pp 1−80.
(26) Koh, Y. P.; Simon, S. L. Structural relaxation of stacked ultrathin polystyrene films. *J. Polym. Sci., Part B: Polym. Phys.* **2008**, *46*, 2741−2753.
(27) Koh, Y. P.; Grassia, L.; Simon, S. L. Structural recovery of a single polystyrene thin film using nanocalorimetry to extend the aging time and temperature range. *Thermochim. Acta* **2015**, *603*, 135−141.
(28) Koh, Y. P.; Gao, S.; Simon, S. L. Structural recovery of a single polystyrene thin film using Flash DSC at low aging temperatures. *Polymer* **2016**, *96*, 182−187.
(29) Simon, S. L.; Koh, Y. P. In *Fast Scanning Calorimetry*; Schick, J., Mathod, D., Eds.; Springer International Publishing, 2016; pp 433−459.
(30) Perez-De-Eulate, N. G.; Cangialosi, D. Double mechanism for structural recovery of polystyrene nanospheres. *Macromolecules* **2018**, *51*, 3299−3307.
(31) Androsch, R.; Schick, C. Interplay between the relaxation of the glass of random L/D-lactide copolymers and homogeneous crystal nucleation: evidence for segregation of chain defects. *J. Phys. Chem. B* **2016**, *120*, 4522−4528.
(32) Monnier, X.; Saiter, A.; Dargent, E. Physical aging in PLA through standard DSC and fast scanning calorimetry investigations. *Thermochim. Acta* **2017**, *648*, 13−22.
(33) Androsch, R.; Schick, C.; Schmelzer, J. W. P. Sequence of enthalpy relaxation, homogeneous crystal nucleation and crystal growth in glassy polyamide 6. *Eur. Polym. J.* **2014**, *53*, 100−108.
(34) Androsch, R.; Zhuravlev, E.; Schmelzer, J. W. P.; Schick, C. Relaxation and crystal nucleation in polymer glasses. *Eur. Polym. J.* **2018**, *102*, 195−208.
(35) Doulut, S.; Bacharan, C.; Demont, P.; Bernès, A.; Lacabanne, C. Physical aging and tacticity effects on the $\alpha$ relaxation mode of amorphous polymers by thermally stimulated techniques. *J. Non-Cryst. Solids* **1998**, *235-237*, 645−651.
(36) Pasztor, A. J., Jr; Landes, B. G.; Karjala, P. J. Thermal properties of syndiotactic polystyrene. *Thermochim. Acta* **1991**, *177*, 187−195.
(37) Polymer Source, Inc. https://www.polymersource.ca/, (accessed Feb 8, 2019).
(38) Scientific Polymer Products, Inc. https://scientificpolymer.com/, (accessed Feb 8, 2019).
(39) Cebe, P.; Partlow, B. P.; Kaplan, D. L.; Wurm, A.; Zhuravlev, E.; Schick, C. Using flash DSC for determining the liquid state heat capacity of silk fibroin. *Thermochim. Acta* **2015**, *615*, 8−14.
(40) Pyda, M. *The Advanced Thermal Analysis System (ATHAS) Databank—Polymer Thermodynamics*; Springer Materials, 2014.
(41) Tool, A. Q. Effect of heat-treatment on the density and constitution of high-silica glasses of the borosilicate type. *J. Am. Ceram. Soc.* **1948**, *31*, 177−186.
(42) Petrie, S. E. B. Thermal behavior of annealed organic glasses. *J. Polym. Sci., Part A-2* **1972**, *10*, 1255−1272.
(43) Koh, Y. P.; Simon, S. L. Enthalpy recovery of ultrathin polystyrene film using Flash-DSC. *Polymer* **2018**, *143*, 40−45.
(44) Greiner, R.; Schwarzl, F. R. Thermal contraction and volume relaxation of amorphous polymers. *Rheol. Acta* **1984**, *23*, 378−395.
(45) Qin, Q.; McKenna, G. B. Correlation between dynamic fragility and glass transition temperature for different classes of glass forming liquids. *J. Non-Cryst. Solids* **2006**, *352*, 2977−2985.
(46) Chen, K.; Vyazovkin, S. Isoconversional kinetics of glass aging. *J. Phys. Chem. B* **2009**, *113*, 4631−4635.
(47) Roe, R.-J.; Millman, G. M. Physical aging in polystyrene: Comparison of the changes in creep behavior with the enthalpy relaxation. *Polym. Eng. Sci.* **1983**, *23*, 318−322.
(48) Ho, C. H.; Vu-Khanh, T. Effects of time and temperature on physical aging of polycarbonate. *Theor. Appl. Fract. Mech.* **2003**, *39*, 107−116.
(49) Hutchinson, J. M.; Smith, S.; Horne, B.; Gourlay, G. M. Physical aging of polycarbonate: enthalpy relaxation, creep response, and yielding behavior. *Macromolecules* **1999**, *32*, 5046−5061.
(50) Pappin, A. J.; Hutchinson, J. M.; Ingram, M. D. Enthalpy relaxation in polymer glasses: evaluation and interpretation of the Tool-Narayanaswamy parameter x for poly (vinyl chloride). *Macromolecules* **1992**, *25*, 1084−1089.
(51) Nakaoki, T.; Kobayashi, M. Local conformation of glassy polystyrenes with different stereoregularity. *J. Mol. Struct.* **2003**, *655*, 343−349.
(52) Takebe, T.; Yamasaki, K.; Funaki, K.; Malanga, M. In *Syndiotactic Polystyrene: Synthesis, Characterization, Processing, and Applications*; Schellenberg, J., Ed.; John Wiley & Sons, Inc.: Hoboken, NJ, USA, 2009; pp 295−307.
(53) Kobayashi, M.; Hanafusa, S.; Yoshioka, T.; Koizumi, S. Molecular form and stereoregularity of polystyrenes in glassy state. *Kobunshi Ronbunshu* **1996**, *53*, 575−581.
(54) Woo, E. M.; Chang, L. *Tacticity in Vinyl Polymers*; Wiley Online Library, 4th ed., 2002; pp 1−22.
(55) Levita, G.; Struik, L. C. E. Physical ageing in rigid chain polymers. *Polymer* **1983**, *24*, 1071−1074.
(56) Yamasaki, K.; Tomotsu, N.; Malanga, M. In *Modern Styrenic Polymers: Polystyrenes and Styrenic Copolymers*; Scheirs, J., Priddy, D., Eds.; Wiley, 2003; pp 389−409.


DOI: 10.1021/acs.macromol.9b01042
*Macromolecules* 2019, 52, 5948−5954